

Thermal imaging of surfaces treated by cooled plasma jet

Abstract. This paper presents the review of methods of plasma temperature decreasing which is performed in atmospheric pressure plasma jet reactors. Special attention is given here to the solution with active cooling system which comprises gas processor and the area of plasma. Non-thermal properties are obtained inside a specifically constructed nozzle which, in this case, serves two functions- that of a zero-potential electrode and the one of an evaporator in a cooling circuit. The produced plasma has much lower temperature than the one produced in nozzle reactors without the cooling system. The experimental part of the paper contains thermal images which show the distribution of temperatures on a surface which is being subject to plasma treatment. Polymer and cellulose were both chosen as representative surfaces.

Streszczenie. W artykule przedstawiono przegląd metod obniżania temperatury plazmy wytwarzanej w reaktorach plazmowych z dyszą, pracujących przy ciśnieniu atmosferycznym. Szczególną uwagę poświęcono rozwiązaniu z aktywnym systemem chłodzenia, który obejmuje gaz procesowy i obszar plazmy. Nietermiczne właściwości, uzyskuje się wewnątrz specjalnie skonstruowanej dyszy, która w tym przypadku pełni równocześnie dwie funkcje: elektrody o potencjale zerowym, oraz parownika w obiegu chłodniczym. Wytwarzana w ten sposób plazma ma temperaturę znacznie niższą, niż powstająca w reaktorach dyszowych bez systemu chłodzenia. Część eksperymentalna artykułu zawiera termogramy obrazujące rozkład temperatur na powierzchni poddawanej obróbce plazmowej. Jako powierzchnie reprezentatywne wybrano polimer oraz celulozę. (Obrazowanie termowizyjne powierzchni plazmowanej przy użyciu chłodzonego reaktora plazmowego typu dyszowego).

Keywords: plasma jet, surface, thermal imaging, active cooling.

Słowa kluczowe: dysza plazmowa, powierzchnia, termowizja, chłodzenie aktywne.

Introduction

Among the applications of non-thermal plasma in biomedicine, there occurs the subject of living structures' treatment in the purpose of influencing the pathogens existing on them. An important parameter, in this case, is the level of plasma temperature which is required to obtain the needed properties of plasma decontamination, and which also influences the stability of discharge products in gas, such as ozone and active gas oxides. At the same time, together with decreasing temperatures of the produced plasma, the negative thermal influence on living tissues is being minimalised. An increased temperature exposes both of the sensitive hydrogen and hydrophobic bonds, causing the protein to lose its spatial structure which is relevant for its function played in living tissues. An exemplary plasma jet reactor is shown in figure 1 and 2.

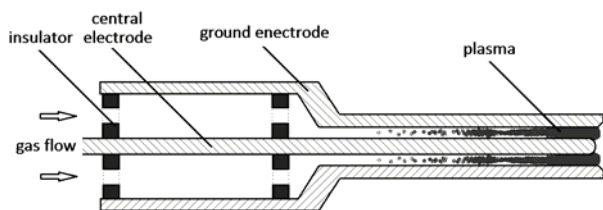


Fig. 1. A cross-section of an exemplary plasma jet.



Fig. 2. Picture of plasma jet created in COMSOL Multiphysics® Modeling Software.

Plasma temperature and temperature decreasing methods

The use of the term of temperature is allowed only when the distribution of energy of kinetic particles composing a specific configuration can be described by a Maxwell

distribution. In the state of thermodynamic equilibrium in plasma, the energy is evenly distributed into all the degrees of freedom of the particles and, eventually, it leads to their mean kinetic energy values being alike [1]. This state is obtained only very rarely as it excludes any directed movement of particles. Such a movement can be caused for example via the occurrence of an external electrical field. Far more often does the situation occur in which plasma only locally exhibits the state of thermodynamic equilibrium. In this state, under the influence of external electrical field, electrons acquire energies that are far greater than the ionic and neutral particle energy. Due to the fact that the exchange of energy between the electrons and ions takes place more slowly than between particles with comparable size and mass, in low-condensed plasma there might persist a state in which Maxwell distribution will be established for electrons and ions separately, while the mean values of both distributions will not be equal. Therefore, the measurement of some values linked with the term of temperature, such as electrons, ions, and the mean temperature of gas, is possible. Regarding the different properties of each of the mentioned particles, in order to measure their temperature, various methods are used. [2, 3, 4]. Similarly, to determine the level of temperature in plasma jet reactors, it is possible to use different methods.

There is also a number of methods used for decreasing temperature in AAPJ (Atmospheric-Pressure Plasma Jet). The easiest way to do that is to increase the stream of working gas which flows through the reactor. A significant change of temperature occurs when the flow acquires turbulent character. A different way is to provide working gases in liquid state, so that the phase transition could happen only in the plasma generator.

Active cooling system

This paper shows an active cooling system involving process gas and plasma area. Non-thermal plasma properties are obtained inside a specially-constructed jet which is made from copper and has two functions at the same time: zero-potential electrode and evaporator in the cooling system. The cross section of the cooling jet is presented in the figure 3.

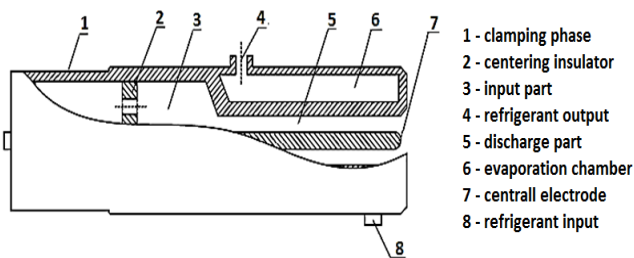
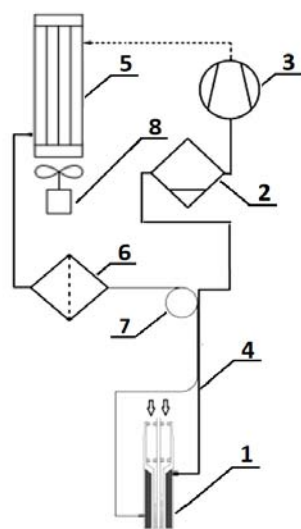


Fig. 3. A cross-section of the cooling jet.

The evaporation chamber is connected to a closed Linde's refrigeration circuit (Fig. 4). In this system the plasma and the refrigerant are not miscible, they are however, powerfully thermally conjoined. Thus, heat migrates from plasma to over-heated steams of refrigerant.



- 1 - plasma jet
- 2 - condensate separator
- 3 - compressor
- 4 - elastic hose
- 5 - condenser
- 6 - dryer-filter
- 7 - capillary tube
- 8 - axial fan

Fig. 4. Diagram of refrigeration cycle designated for plasma jet.

As a refrigerant, 1,1,1,2 tetra-fluoro-ethane, known under the trade name R134a, was used. The refrigerant, in liquid form, was introduced into the ring-shaped cooling chamber located inside the plasma jet. Relative pressure in the nozzle cooling chamber was -0.02 MPa. Due to such low pressure, a rapid boiling and evaporation of the refrigerant occurred. Due to small geometry of the evaporator and the discharge area and the significant thermal conductivity of the nozzle, the energy of the phase transition enthalpy was absorbed from the resulting plasma to the superheating vapor of the refrigerant.

High frequency power supply

The plasma jet was supplied by sinewave voltage of 14.84 MHz in the way that the sinewave signal was delivered to the high-frequency amplifier and was amplified to $50V$. Next, the signal was passed to the air coreless transformer which had a turn ratio of $1/10$. The secondary

side of transformer was connected to the plasma jet and simultaneously, the resonant capacitor was also placed there. The frequency was adjusted to obtain as low a reactive power as possible, in this case it was 14.84 MHz with the value of active power equal to $50W$. During the process of changing frequencies into higher or lower values than the given one, the reactor refrained from being properly supplied. The block diagram of power supply system is presented in figure 5.

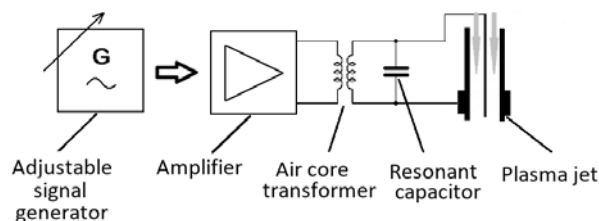


Fig. 5. Block diagram of plasma jet power supply system.

Thermal imaging

Two materials were selected for plasma processing. In the first case it was a popular acrylonitrile butadiene styrene polymer (ABS) sample of thickness 2 mm.

In the second case, the plasma treatment was carried out on 120 g/mm² white paper.

Thermal imaging was conducted with the use of camera VIGOCam V50 and the edition of images was conducted in a Therm 2.21.2 environment. Before the conduction of the measurement the camera had adjustments of emission factors set. This selection was made according to standard procedures: the temperature of the surface was heated in a homogenous way, next the surface temperature was measured with the use of thermocouple and the emission factor was adjusted so that the thermal image surface of temperature indication was the same as the one indicated by thermocouple.

Before the beginning of appropriate measurements, the air temperature was measured and it was in the range of 22 to 23 °C. Humidity was also measured and it was equal to 63% . For the ABS material the emission factor was established on the level of 0.990 and for the paper - 0.945 . The average distance between the surface and the camera lens was equal to 540 mm.

The reactor worked with helium and nitrogen gases with volume streams 7.1 m³/min and 4.1 m³/min. This situation is presented on figure 6. Additionally, figure 7 shows the camera-eye view of plasma jet and surface before the treatment. This image is not of good quality but it shows the contours, and the relative placement of what is on the post.

The polymer plate was plasma-treated until the arrest in changes of the observed field of surface temperature and the image was saved. Next, the cooling system was started and the change of the temperature was being observed until its halt and the images were saved subsequently. Due to the fact that thermal images have the inadequacy of concerning the surface, not the nozzle, they were arranged in the way that they began from 0 °C. However, in every case of cooling in this paper, in constant conditions, the temperature of the nozzle was equal to -22.7 °C. Although it is not visible in the thermal images provided here, it is not of our main interest, as the paper aims to prove the efficiency of the cooling system and to show the decrease of surface heating.

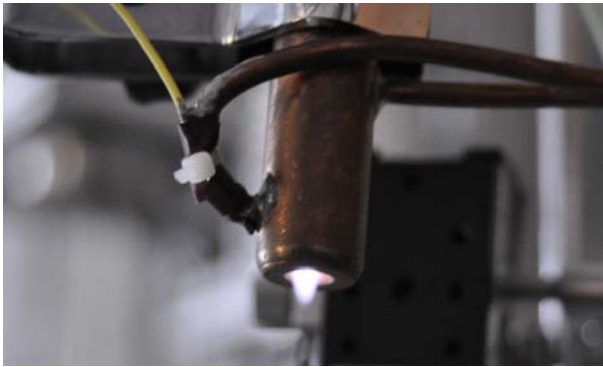


Fig. 6. Plasma jet which is working for 50W of power and nitrogen - helium conditions.

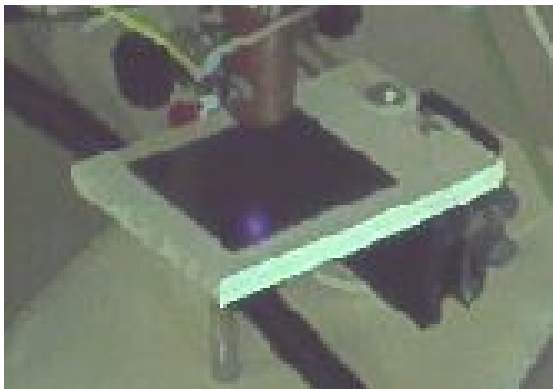


Fig. 6. A camera-eye view of laboratory work station with plasma jet.

Thermal images

During the main part of the experiment, the plasma reactor was stationary and was placed both vertically and perpendicularly above the treated surface. The distance between the reactor and the surface was equal 25 mm.

The reactor was switched on and the temperature fields were noticed to stabilize. The obtained thermogram was shown on figure 7.

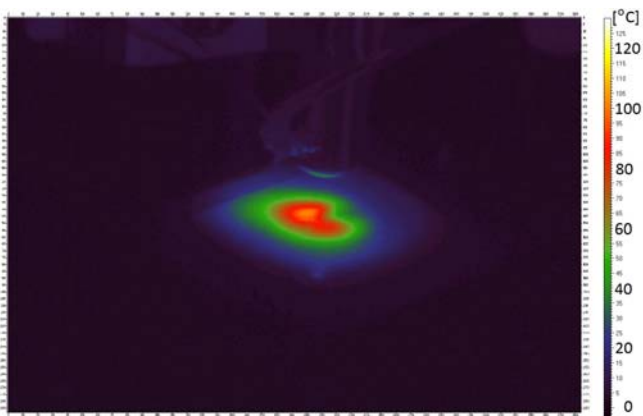


Fig. 7. A thermal image of plasma treated ABS surface by *plasma jet* reactor without cooling for nitrogen and helium conditions

Next, the cooling system was started and the change of the temperature was being observed until its halt and the images were saved, as shown in Fig. 8.

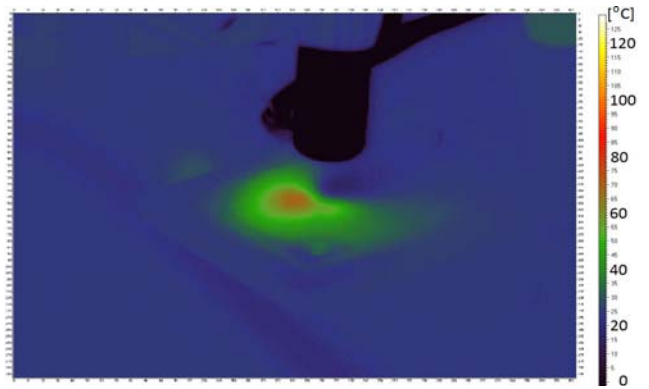


Fig. 8. A thermal image of plasma treated ABS surface by plasma jet reactor with working cooling system for nitrogen and helium conditions.

This part of treatment was repeated for the paper surface. The obtained thermogram with deactivated colling is shown on figure. 9.

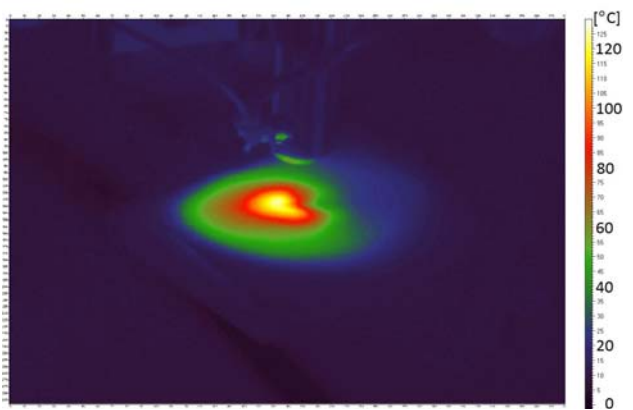


Fig. 9. A thermal image of plasma treated paper surface by *plasma jet* reactor without cooling for nitrogen and helium conditions

The treatment was repeated for the running cooling system (Fig. 10). After the main plasma treatment, the comparative measurement was performed.

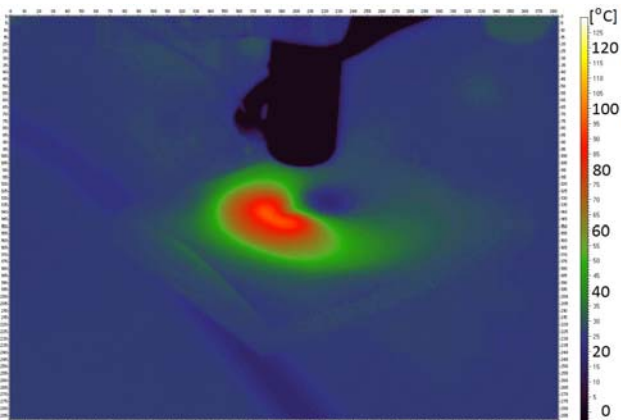


Fig. 10. A thermal image of plasma-treated paper surface by plasma jet reactor with working cooling system for nitrogen and helium conditions.

During this comparative measurement the same gas mixture was delivered to the plasma jet. The cooling system was working continuously but the electrical power was not delivered and electrical discharge did not exist. After that,

the temperature fields were noticed to stabilize. The obtained thermogram was shown on figure 11.

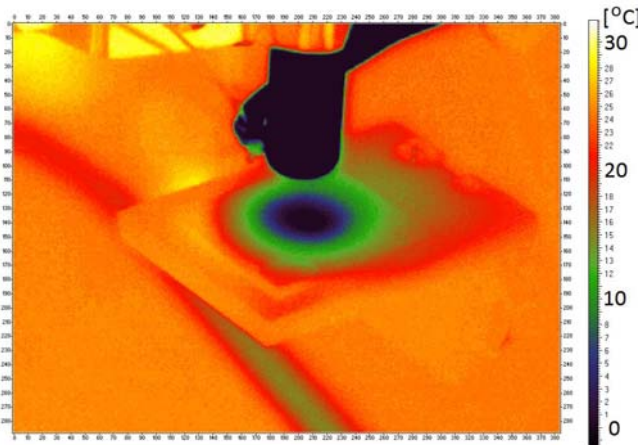


Fig. 11. A thermal image of ABS surface placed under the plasma jet reactor with working cooling system for nitrogen and helium conditions during the comparative measurement.

Summary

The surface of polymer in the central point under the reactor usually reached the highest temperatures, and for the ABS it exceeded 117 °C. It was observed that the surface of the sample, while heavily heated, lost its shape and the temperature field was not distributed radially. It is visible on thermal image and its shape is non-circular and irregular. In the hottest point the temperature was 127 °C and the area above 100 °C had the surface of 170 mm². After starting the cooling system a significant temperature change was observed. The temperature of the hottest point was 82,5 °C and it is a decrease of 34,5 °C. The results for polymer ABS enable to draw the conclusion that the cooling is efficient. The trial was repeated for paper surface of white color. It was observed, due to its low mass, that the paper does not create a perfectly flat surface and the distribution of temperature field is accordingly deformed, if compared to the expected one. On thermal image without the cooling system the highest temperature was observed, namely 131 °C. However, after cooling down, it dropped down to 94 °C. The decrease of temperature is over 35 °C. It also confirms the efficiency of the cooling system. Lastly, a control treatment was conducted, during which, for the

same gas flows, electric power was shut down, but the cooling was on. Then, the surface temperature in its coolest point was on the level of 3 °C.

The research proved the cooling system to be highly efficient which is visible on both - thermal images. The temperature of the treated plate was decreased up to 35 °C degrees Celsius and the result is unobtainable for any other known cooling methods. The proposed solution shows an applicatory potential not only in medical and biotechnological fields, but also during the treatment of high-temperature-susceptible materials which are represented by a low threshold of thermal plastification. The thermal imaging method does not provide very precise measurements, but it gives a good view on the distribution of the temperature on surface. In order to measure it precisely, at least two different methods should be used, based on two different physical phenomena. Nonetheless, relevant trends can be observed in this kind of measurement.

Authors: mgr inż. Piotr Krupski, Politechnika Lubelska, Wydział Elektrotechniki i Informatyki, Instytut Elektrotechniki i Elektrotechnologii, ul. Nadbystrzycka, 38a, 20-618 Lublin, E-mail: piotr-ij@o2.pl, Prof. dr hab. inż. Henryka Danuta Stryczewska, Politechnika Lubelska, Wydział Elektrotechniki i Informatyki, Instytut Elektrotechniki i Elektrotechnologii, ul. Nadbystrzycka, 38a, 20-618 Lublin, E-mail: hdstryczewska@wp.pl

REFERENCES

- [1] Terebun P., Krupski P., Kwiatkowski M., Samoń R., Diatczyk J., Pawłat J., Stryczewska H. D.: Wybrane metody pomiaru temperatury plazmy w reaktorach typu jet, *INFORMATYKA, AUTOMATYKA, POMIARY W GOSPODARCE I OCHRONIE ŚRODOWISKA*, Tom 3, 2015,
- [2] Diatczyk J., Stryczewska H. D., Komarzynec G.: Modeling of the Temperature Distribution in Arc Discharge Plasma Reactor, *JOURNAL OF ADVANCED OXIDATION TECHNOLOGIES*, Vol. 9, no 2, July 31, 2006,
- [3] Mahmood S., Shaikh Nek M., Kalyar M. A., Rafiq M., Piracha N. K., Baig M. A.: Measurements of electron density, temperature and photoionization cross sections of the excited states of neon in a discharge plasma. *JOURNAL OF QUANTITATIVE SPECTROSCOPY AND RADIATIVE TRANSFER*, 110 (17), 2009,
- [4] Stryczewska H. D., Diatczyk J., Pawłat J.: Temperature distribution in the gliding arc discharge chamber, *JOURNAL OF ADVANCED OXIDATION TECHNOLOGIES*, Volume 14, Number 2, July 2011.